

Synthesis and Characterization of Alumina Based Porcelains Insulator using Economical Raw Materials Doped with Zirconia

5.1 Introduction

Ceramic oxide materials play an crucial role in the region of mechanical and electric applications for many years due to its unique properties such as high thermal stability, high dielectric constant, low electrical conductivity and high resistivity [Huang et al. 2005 and Štubňa 2009]. The high-voltage ceramic electrical porcelain is one of the most essential components of the electrical grid. The microstructure strongly influences mechanical properties, and it is observed that microcracks are observed around the quartz grains at room temperature, which arises during the β to α transformation of unsolved quartz grains.

However one of the main drawbacks of alumina-based porcelain insulator is its low fracture toughness that may limit its use in high mechanical applications. Because cracks easily propagate in alumina ceramics; thus, they fail unexpectedly in service [Olupot et al. 2010, Touzin et al. 2010 and Gralik et al. 2014]. One of the approaches to increase its fracture toughness is to incorporate a second phase that interacts with alumina boundaries to improve the toughness markedly. ZrO_2 has been used extensively as a second phase with alumina ceramics. The effect of alumina doping on zirconia grain conductivity is found to be very low, while grain boundary conductivity decreases significantly [Meng et al. 2016, M'Peko et al. 2003 and Tartaj et al. 1996].

In chapter 4, we analysis the effect of zirconia (0 to 30 wt. %) addition on Physico-Mechanical and dielectric properties of porcelain insulator. The addition of ZrO_2 to alumina-based ceramic promotes the densification and electro mechanical properties of ceramics porcelain insulator [Guo et al. 1995 and Wahsh et al. 2012]. Zirconia is expensive according to economical point of view so our aim is to decrease the concentration of zirconia. For that purpose we take a composition A3 (from previous chapter 3) and adding zirconia concentration (from 0 to 10 wt. %). The whole purpose of the present studies is to understand the effect of sintering behavior on physical, electrical, mechanical, thermal and dielectric properties of alumina-based porcelain after doped with zirconia concentration (0 to 10 wt.%). Alumina-zirconia ceramic composites using in refractory and high-temperature applications where severe thermal shock with high mechanical features as well as for its fascinating applications in power and transmission industry.

5.2 Experimental Details

5.2.1 Material and Preparation

For the preparation of porcelain composition doped with zirconia, containing raw materials like ball clay, kaolin, feldspar, silica, and alumina were formulated in Table 5. 1: Batch codes with their composition (weight %).Table 5. 1. Particle size distribution of raw materials is shown in

Table 5. 2. Further, the detailed description for experimental procedure shown in chapter 2 (section 2.2). Different shapes of moulds are used for making various shaped samples using a uniaxial pressing was done by a hydraulic press at a pressure of 160 MPa, for a) Rectangular

Chapter 5: Synthesis and Characterization of Alumina Based Porcelains Insulator using Economical Raw Materials Doped with Zirconia

(40 mm x 10 mm x 10 mm), b) Square (25 mm x 25 mm), c) Circular (15 mm and 10 mm diameter) shown in Figure 5. 1.

Table 5. 1: Batch codes with their composition (weight %).

Batch codes	Ball clay	Kaolin	Feldspar	Silica	Alumina	Zirconia
D 1	20	25	10	10	35	0
D 2	20	25	10	10	32.5	2.5
D 3	20	25	10	10	30	5
D 4	20	25	10	10	27.5	7.5
D 5	20	25	10	10	25	10

Table 5. 2: Particle size distribution of raw materials.

Raw materials	Particle size ($\leq \mu\text{m}$)
Kaolin	120
Feldspar	100
Silica	80
Alumina	80
Zirconia	80

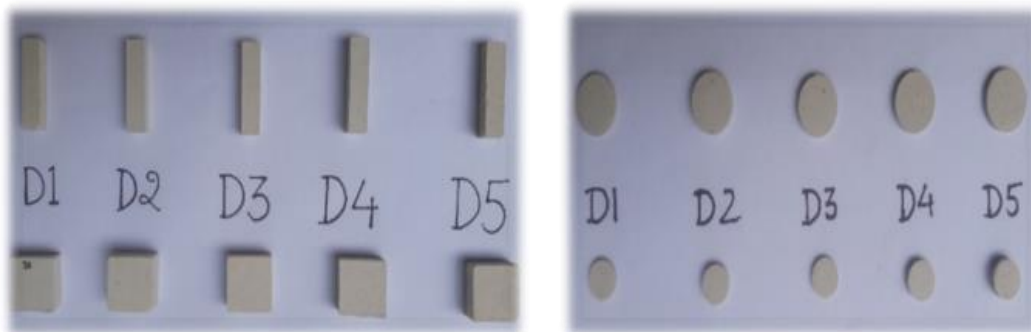


Figure 5. 1: Prepared samples of different compositions sintered at 1350°C with their batch codes.

The prepared samples of having different compositions (D1, D2, D3, D4, and D5), sintered at 1350°C with heating rates of 5°C per minute with a soaking period of 2 hours at the said temperature (Figure 5. 1).

5.2.2 Characterizations

Various techniques were used to investigate the physical, electrical, mechanical, thermal and morphological characteristic of sintered samples. For physical behavior, densification parameters such as bulk density (B.D) and apparent porosity (A.P) of the sintered samples of all the porcelain composition were determined by Archimedes method according to ASTM C20-00. Linear shrinkage was measured according to the method described by ASTM C356-10. The thermal behavior of each composition was determined by dilatometer analysis (M/s V.B Ceramics and consultant, Chennai, India).

5.2.3 X-Ray Diffraction (XRD) Analysis

The phase compositions of prepared samples were identified by X-ray diffraction (XRD) (Serial no: HD20972, Rigaku Corporation, Tokyo, Japan) with Cu-K α radiation ($\lambda = 1.54056 \text{ \AA}$) and a Ni filter, a working voltage of 40 kV, and a working current of 30 mA. The samples were scanned in the 10 to 80° (2 θ) intervals at a scanning speed of 5°/minute.

5.2.4 Scanning Electron Microscopy (SEM) Analysis

The microstructure of sintered prepared sample surfaces was determined using an SEM (Zeiss Company Model No. Evo\18-2045, Tokyo, Japan) working at 20 kV as an accelerating voltage. All samples having different composition were coated before their analysis by SEM.

5.2.5 Mechanical Tests

The modulus of rupture (MOR) or bending strength measurement was performed on the Universal Testing Machine (FINE TFUC sales and services instrument, India). A rectangular specimen (45 mm x 10 mm x 10 mm) is required for the three-point bending test. The sample is placed between two supports which are 40 mm apart (L), and at the exact middle of the two support (L/2) force (F) applying with the speed of 2 mm/min. The maximum load of fracture was noted, and modulus of rupture (MOR) was obtained as follows:

$$\text{MOR} = \frac{3FL}{2bt^2}$$

Where F is the load at failure (N), L is the distance between supports, b is the sample breadth, and t is the thickness of the sintered sample.

For tensile strength testing of porcelains samples was obtained by using a Universal Testing Machine (UTM). Four samples were prepared from each composition, then take an average value of each sample. Samples were having dimension 25mm gauge length, 7mm width, 10mm thickness and 40mm overall length. The prepared rectangular sample is compressed between flat plates. The tensile strength of the samples is obtained by following relation:

$$\sigma_t = F / A$$

Where σ_t (MPa) is the maximum tensile stress, F (in N) is the applied load at fracture; A (mm^2) is the cross-sectional area.

5.2.6 Electrical Tests

To perform the electrical measurements, the samples were polished to obtain parallel surfaces and placed between the two parallel plates. The electrical properties such as AC dielectric constant (ϵ'), dielectric loss factor (ϵ''), dielectric loss tangent ($\tan\delta$), conductivity and

resistivity were measured using an Impedance network analyzer (Keysight Technology, model-E4990A, Malaysia) at frequencies between 20 Hz and 20 MHz. Samples are having a thickness ≤ 2 mm and diameter ≤ 10 mm were used for this test. The samples were coated on both sides with silver to make capacitor of the samples and placed between the plates and measured the value of the capacitor.

$$C = \frac{\epsilon_0 \epsilon' A}{t}$$

Where ϵ_0 is permittivity of free space (8.85×10^{-12} F/m), A is the area of the samples and t thickness of the samples.

For measurement of AC dielectric constant and dielectric loss at microwave frequency (1 to 20 GHz) is analyzed using vector network analyzer.

5.3 Result and Discussion

5.3.1 X-Ray Diffraction

The XRD patterns of different samples are having zirconia content (0, 2.5, 5, 7.5 and 10 wt. %) and sintered at 1350°C are shown in Figure 5. 2. The qualitative analysis results show that the samples are mainly composed of corundum (PDF 46-1212), mullite (PDF 79-1456), m-zrO₂ (PDF 65-1024), zircon (PDF 83-1374), cristobalite (PDF 39-1425) as well as amorphous phase. As the concentration of zirconia increased, and alumina decreased, the major peaks intensity decreased at an angle (2θ) of 25°, 35°, 43° and 57° corresponding to alumina (#) because of the dissolution of alumina into glassy phase at high temperature. At the same time, there is a little enhance in the intensity peaks (t and m-ZrO₂ and zircon) of the samples (D2, D3, D4, and D5). The formation of zircon is due to the solid-state reaction

between tetragonal zirconia and silica (amorphous and cristobalite). Below 900°C the powder is found to be amorphous, whereas the crystallization of t- ZrO₂ was observed at 900°C. The phase transformation in zirconia powder from metastable tetragonal to monoclinic ZrO₂ is usually in the range of 600 to 1000°C. Above 1100°C, it in the tetragonal phase [Kanno 1989]. Therefore, the zirconia phase involved in the zircon formation is always the tetragonal one, and any consideration on the nature of the zirconia phase included in the zircon formation is from amorphous powders, like that reported by Y Kano, 1989.

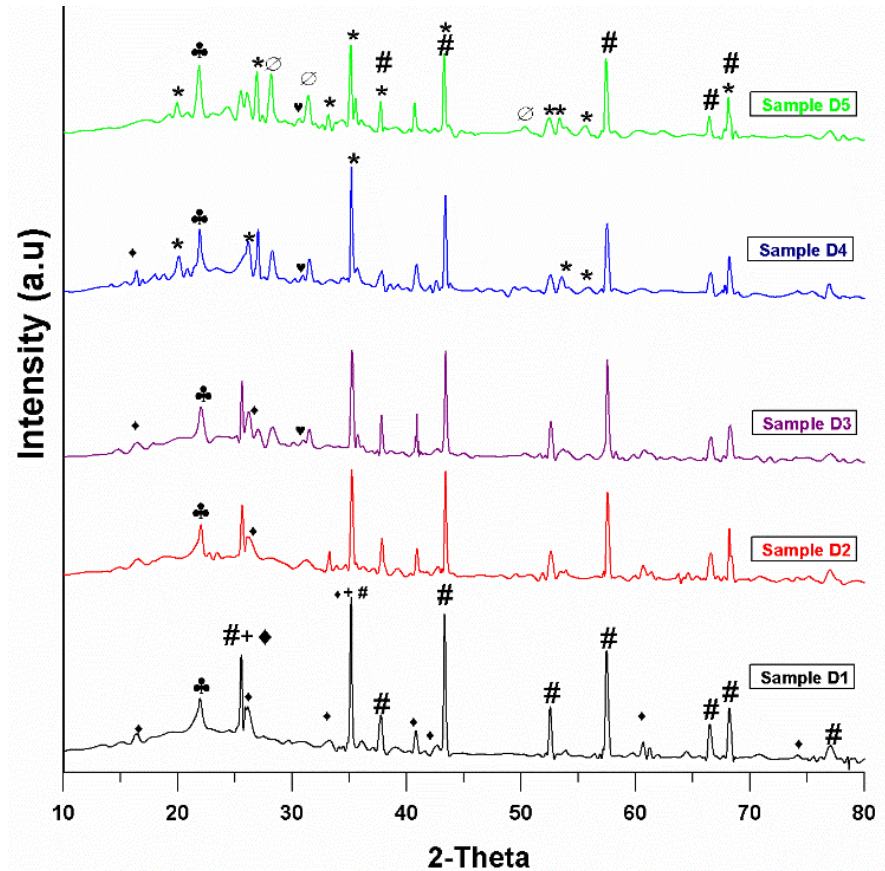


Figure 5. 2: XRD pattern of samples (D1, D2, D3, D4 and D5) sintered at 1350°C; #: corundum; ♦: mullite; ♣: cristobalite; *: ZrSiO₄; ∅: m-ZrO₂ and ♥: t- ZrO₂.

The cristobalite phase is developed at significant peak intensity in all samples at 21.9° with *h, k, l*, values of (1, 0, 1) and having a tetragonal structure with space group P4₁2₁2. The intensity of cristobalite in sample D5 is higher than that of the other sintered samples. The estimation of particle size is done using Debye Scherer formula, which is given by

$$D = \frac{0.9\lambda}{\beta \cos \theta}$$

Where D is the particle size or crystallite size, β= Full width half maximum intensity (FWHM) of highest peak and λ is the wavelength of the X-ray. The crystallite size of the different sintered samples (D1, D2, D3, D4, and D5) listed in Table 5. 3.

Table 5. 3: Show the crystallite size of sintered samples at 1350°C with a soaking period of 2 hours.

Samples	Peak intensity (2θ)	β	Crystallite Size D (nm)
D1	35.2	0.182	0.7993
D2	35.2	0.242	0.6026
D3	35.2	0.225	0.6476
D4	35.2	0.283	0.5152
D5	35.2	0.261	0.5588

5.3.2 Scanning Electron Microscopy

Figure 5. 3, Shows the SEM micrograph of five different compositions sintered at 1350°C. The surface topographies confirmed the presence of little agglomeration and porosity in the samples. The pore size, shape and distribution, as well as total porosity, are of great importance on the property of insulators. Most of the pores in samples are various in shape

such as circular, elliptical and irregular, with the average size of $\leq 2.5\mu\text{m}$, and homogeneously distributed in the body. There rarely exists interconnected pore or large pore.

Table 5. 4: Shown the average grain and pore size of the samples.

Samples	D1	D2	D3	D4	D5
Grain Size (μm)	1.44	1.59	1.63	2.19	1.59
Pores Size (μm)	2.29	1.43	1.11	1.14	1.32

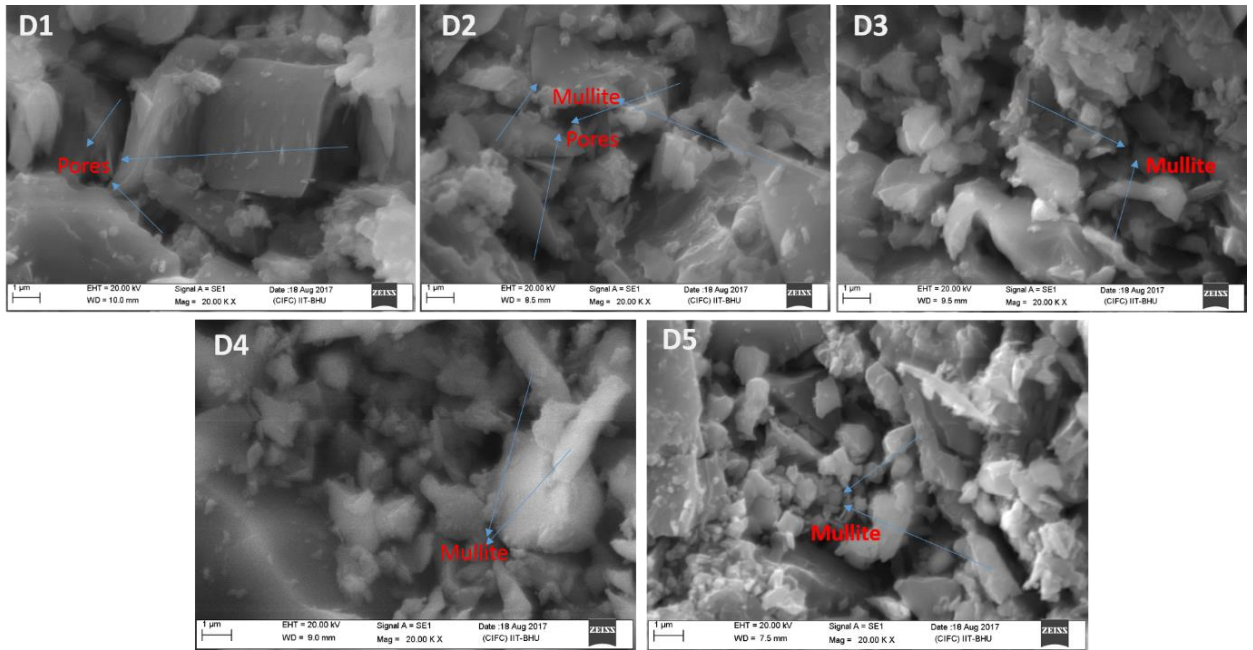


Figure 5. 3: SEM micrograph of the different samples (D1, D2, D3, D4 and D5) was investigated.

The porosity of all five different compositions having ZrO_2 (0 to 10 wt. %) concentration is measured by Archimedes method are listed in Table 5. 5. The total average apparent porosity of all the samples measured is 1.44% listed in Table 5. 5. The average pores and grain size

of all the sintered (1350°C) samples measured using image J software were listed in Table 5.4.

5.3.3 Coefficient of thermal expansion

The coefficient of thermal expansion (CTE) of material gives a prior impression about its service life when exposed to a higher temperature environment. Prior knowledge of CTE of the materials would subsequently, assist to design the component to enhance its service life. From the slope of the coefficient of thermal expansion (α) has been measured under different temperature range (30 to 1350°C using dilatometer at a heating rate of 5°C/min. CTE of composition was measured from ambient temperature to 1300°C by using formula.

$$\alpha = \frac{\Delta L}{L \Delta T}$$

Where L is the length of the test sample and ΔL is the change in length at ambient temperature from ambient temperature to 1300°C, ΔT is the change in temperature. From Figure 5.4, it showed average negative expansion for all samples is 190°C followed by positive expansion up to 1350°C. Approx. 1050°C the samples showed start to negative expansion, due to the start of densification. From Figure 5.4, it reveals that CTE of the different composition decreases as we increase the concentration of zirconia (sample D2, D4, and D5). The coefficient of thermal expansion (α) has been measured under different temperature range and then averaged over the complete temperature range to evaluate α_{avg} of the samples from 250°C to 450°C, and 1050°C to 1250°C is measured to be $8.254 \times 10^{-6}/^{\circ}\text{C}$ and $7.16 \times 10^{-6}/^{\circ}\text{C}$. The change in nature of the plot at high temperature may be attributed to the change in microstructure or phase during heating [Nath et al. 2015]. Thermal expansion decreases due

to increasing bond energy, which affects the melting point of solids, so high melting point materials to have lower thermal expansion.

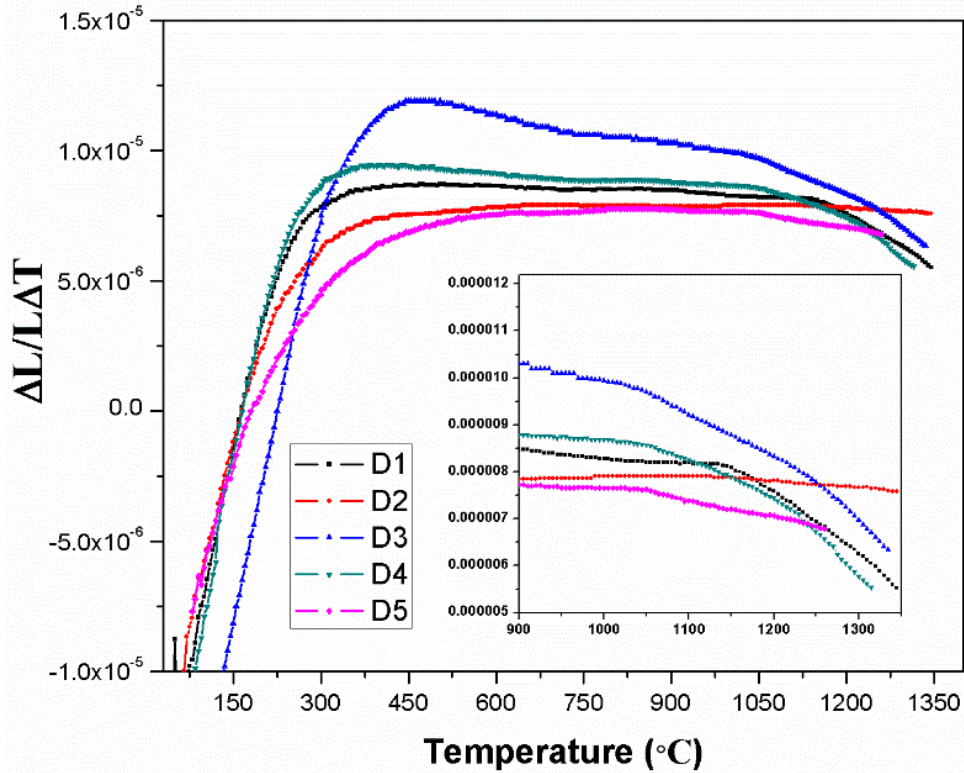


Figure 5. 4: Variation of the coefficient of thermal expansion with temperature after addition of zirconia (0 to 10 wt. %) content in porcelain composition.

5.3.4 Physical and Mechanical Behaviour

Figure 5. 5, shows the bulk density and apparent porosity values of different samples sintered at 1350°C. All the samples showed increased densification on the addition of zirconia up to 7.5 wt % in base composition. This densification proceeded due to the grain boundary diffusion and also densification results were confirmed by measuring the linear shrinkage (L.S) of the compacts samples sintered at 1350°C. The water absorption (W.A) of samples

decreased with increasing zirconia addition because bulk pores (close and open pores) in the samples were reduced, glassy phase filled these bulk pores. For high voltage electrical ceramic porcelain insulator water absorption should be minimal or zero, its leads the electrical resistance properties of the body. Further, the value of W.A also decreased by using the glaze on the surface of the samples. From Table 5. 5, it depicts that W.A and A.P dropped to a minimum by addition of 7.5 wt. % ZrO_2 with 27.5 wt. % Al_2O_3 in the base porcelain composition sintered at $1350^\circ C$. The maximum bulk density (2.63 g/cm^3) with also maximum linear shrinkage (8.90 in %) were obtained for above said composition (D4), shown in Table 5. 5.

The maximum observed mechanical strength in samples (D4) such as the bending strength (B.S), tensile strength (T.S) and compressive strength (C.S) values of porcelains sintered at $1350^\circ C$ for 2 hours were 2.63 g/cm^3 , $141 \pm 5 \text{ MPa}$, $40 \pm 3 \text{ MPa}$ and $216 \pm 10 \text{ MPa}$, respectively shown in Figure 5. 6.

Table 5. 5: Physical properties of different composition (D1, D2, D3, D4 and D5) with zirconia wt. % sintered at $1350^\circ C$.

Samples sintering at $1350^\circ C$					
Wt.% ZrO_2	D1	D2	D3	D4	D5
B.D (gm/cc)	2.55	2.58	2.59	2.63	2.60
A.P %	1.88	0.87	0.70	0.47	3.280
L.S %	8.67	8.70	8.85	8.90	8.72
W.L	6.85	6.55	6.52	6.44	7.73
W.A %	0.94	0.34	0.27	0.18	1.30

The compressive strength showed higher values than that of MOR, due to the difference in stresses distribution. After further addition of ZrO_2 (10 wt. %) content, i.e. sample D5, its physical and mechanical strength goes to decline, due to the nonbonding additional zirconia content dispersed at the surface of samples which leads the porosity.

It also conforms to XRD pattern (Figure 5. 2) that the presence of cristobalite phase of silica content in the samples. As we increase the ZrO_2 concentration the cristobalite phase intensity at an angle ($2\theta = 21.9^\circ$) for sample D5 is higher as compared to other samples. At high temperature, there is a formation β cristobalite phase of silica. During the cooling process, the solidification of the vitrified region is later than that of the area around it. The vitrified area will contract when cooling from the liquid state, but there is no enough melt to offset the volume reduction caused by cooling since the area around the melting area is solidified.

It also conforms to XRD pattern (Figure 5. 2) that the presence of cristobalite phase of silica content in the samples. As we increase the ZrO_2 concentration the cristobalite phase intensity at an angle ($2\theta = 21.9^\circ$) for sample D5 is higher as compared to other samples. At high temperature, there is a formation β cristobalite phase of silica. During the cooling process, the solidification of the vitrified region is later than that of the area around it. The vitrified area will contract when cooling from the liquid state, but there is no enough melt to offset the volume reduction caused by cooling since the area around the melting area is solidified. As a consequence, inner-stress causes the appearance of cracks. As for crack around quartz particle, the reason is that there exists a significant β - α phase transformation of quartz particle at $573^\circ C$ during the cooling process. As a result, inner-stress developing the cracks around

the quartz particle. So according to the physical and mechanical properties, the composition having 7.5 wt. % zirconia on base composition showed the maximum values.

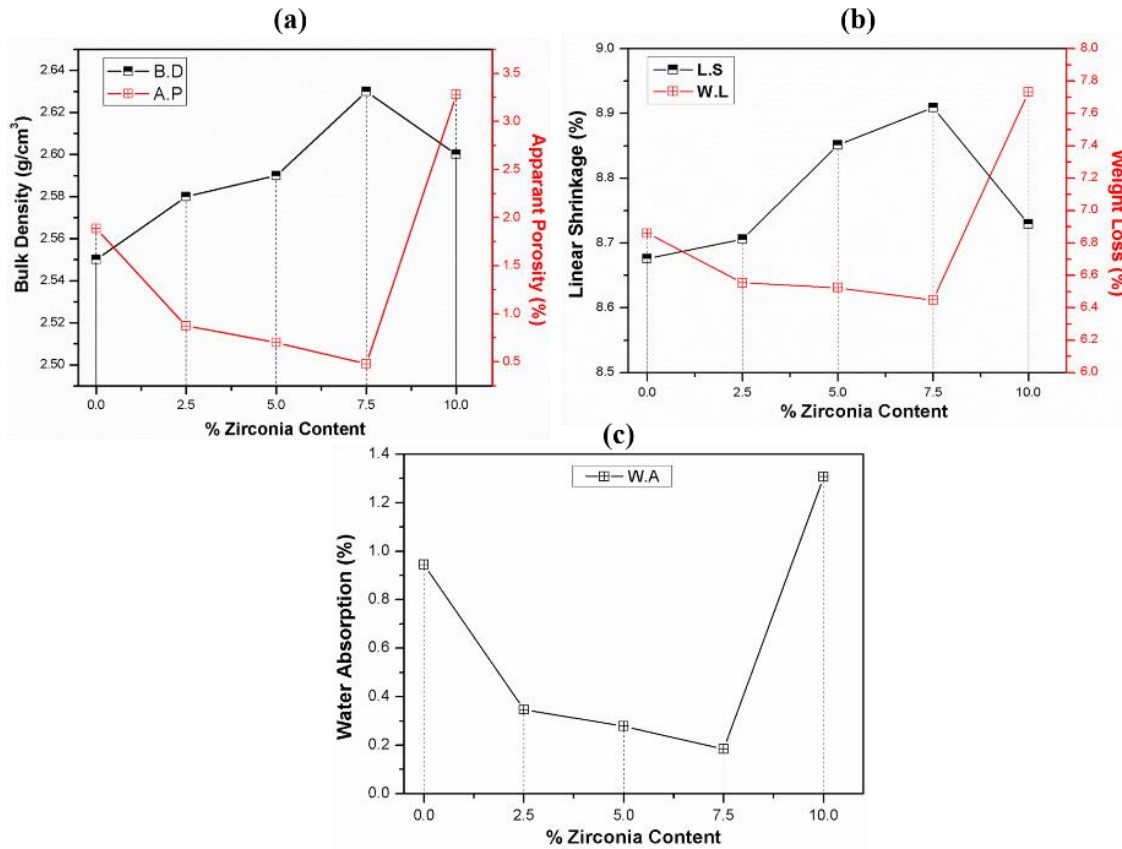


Figure 5. 5: Graph between B.D (in g/cc), A.P (in %), L.S (in %), W.L (in %) and W.A (in %) with content of zirconia (0–10 wt. %) sintered at 1350°C with soaking period for 2 hours.

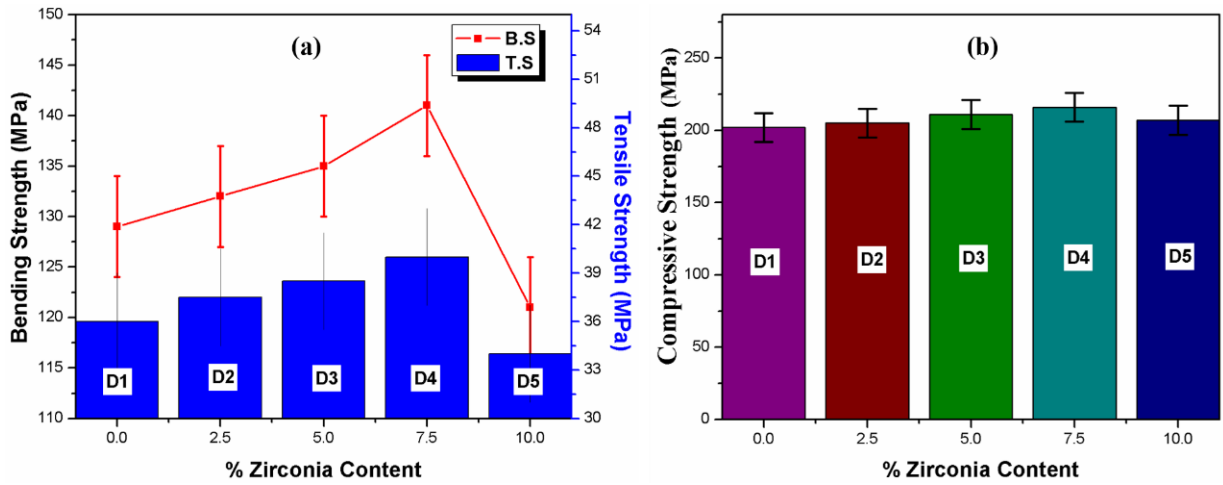


Figure 5. 6: Graph between B.S, T.S and C.S (in MPa) versus zirconia wt. %, for the samples sintered at 1350°C.

5.3.5 Electrical Behaviour

The AC dielectric constant (ϵ') and dielectric loss versus frequency with zirconia addition (wt. %) is plotted in Figure 5. 7. The AC dielectric permittivity (ϵ) is a complex number having real and imaginary parts. The real part is due to the polarization of material, and the imaginary part is associated to Ohmic and polarization losses.

$$\epsilon = \epsilon' - j\epsilon''$$

$$\text{Tan}\delta = \epsilon''/\epsilon'$$

Where ϵ'' is the dielectric loss factor and $\text{tan}\delta$ is the loss tangent or dielectric loss of the material

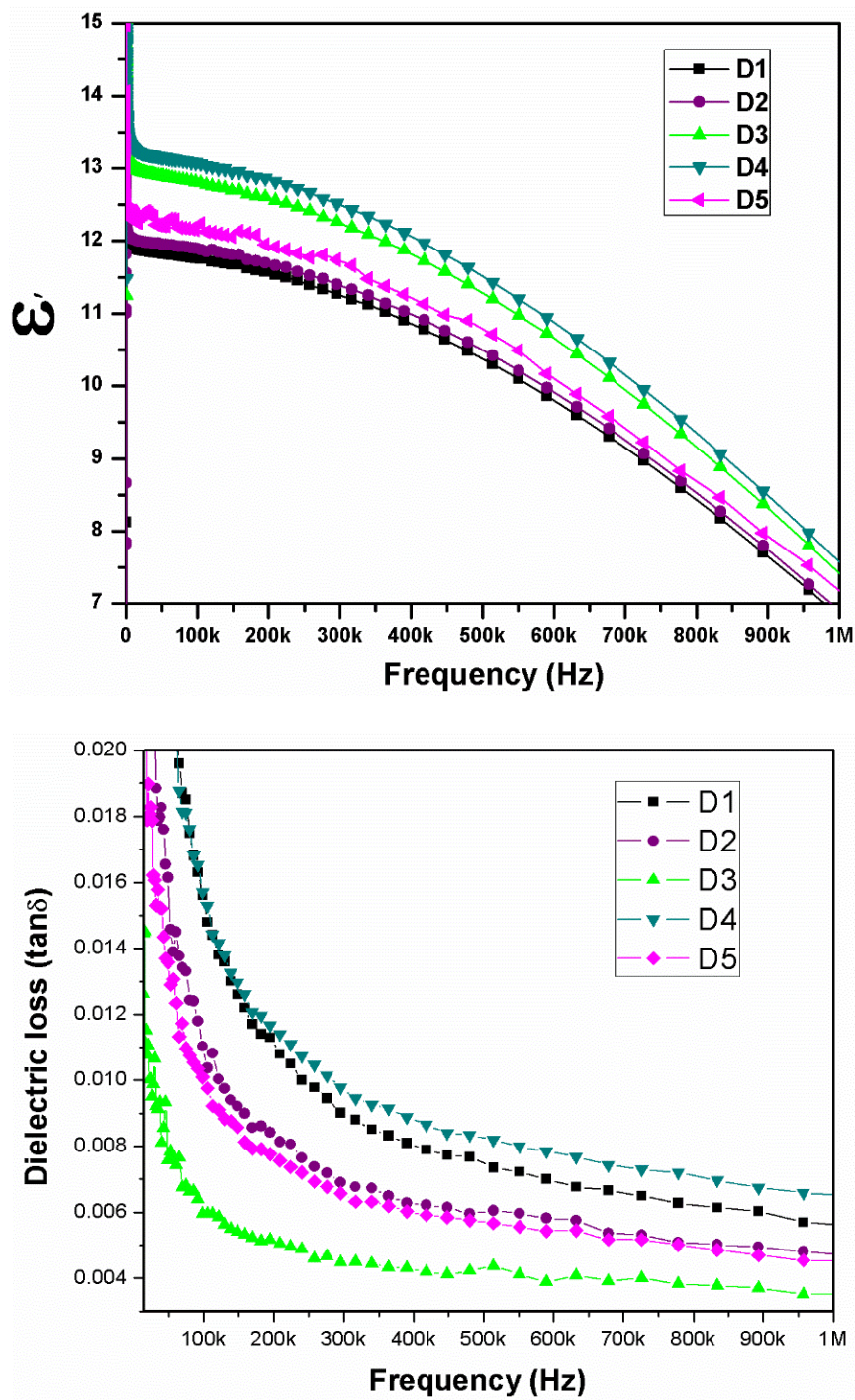


Figure 5. 7: Dielectric constant (ϵ') and loss versus frequency (in Hz) for all the sample sintered at 1350°C (where notation k~10³ and M~10⁶).

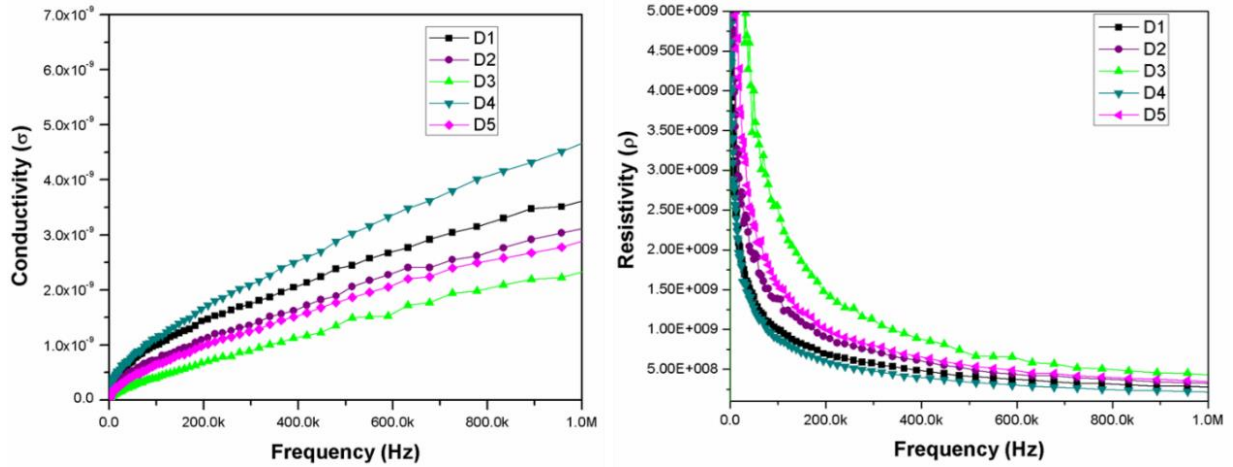


Figure 5. 8: Resisitivity and conductivity versus frequency (in Hz) for all the sample sintered at 1350°C (where notation k~10³ and M~10⁶).

From Figure 5. 7, the dielectric constant value was noticed to increase with the addition of zirconia concentration (up to 7.5 wt. %) and reduce the content of alumina (from 35 to 27.5 wt. %).As we know that the ϵ' value of zirconia (≈ 27), which is better than that of alumina (≈ 10).A value of dielectric depends on the presence of dipoles. If dipoles are there, then it would allow the flow of electrons to reduce the resistance, and hence small dielectric. As the material is compact or dense, it offers more resistance to the flow, therefore dielectric constant is high. So increasing the zirconia content in the porcelain composition, it leads densification of resultant material, increasing ϵ' . The calculated value of dielectric and loss was listed in Table 5. 6.

It is also observed that as we increase the frequency range (100Hz to 1 MHz), the dielectric constant and loss decreases. As we know that the value of dielectric constant mainly depends on three types of polarization effects, i.e. Ionic, orientation and electronic polarizations. Ionic and orientation polarization area slow to process, and it contributes to low frequency, and electronic polarization is fast process exists only at high frequency (in GHz). Therefore, the

electronic polarizability would not change in low frequency (up to MHz), but the ionic polarizability decreased with the increase of the range of frequency [Wan et al. 2015].

Table 5. 6: The dependence of dielectric constant tangent dielectric loss ($\tan\delta$) on the frequency (Hz) and addition of zirconia wt. % for the samples sintered at 1350°C.

Freq. (Hz)	Where $k=10^3$ and $M=10^6$				
	D1	D2	D3	D4	D5
	ϵ'	ϵ'	ϵ'	ϵ'	ϵ'
100	21.32	19.43	19.88	22.42	21.73
10K	12.15	12.16	13.33	13.61	12.49
100K	11.91	12.02	13.01	13.28	12.39
1M	8.17	8.26	8.88	9.06	8.46
	$\tan\delta$	$\tan\delta$	$\tan\delta$	$\tan\delta$	$\tan\delta$
100	1.400	1.230	0.050	1.787	0.159
10K	0.052	0.041	0.014	0.050	0.027
100K	0.015	0.011	0.005	0.015	0.010
1M	0.005	0.004	0.003	0.006	0.004

The eddy current loss mainly depends on the electrical resistivity of the ceramic porcelain insulator. So, it may be considered that lowering the value of dielectric loss in porcelain results mainly from a reduction in eddy current loss due to their higher electrical resistivity. The calculated value of resistivity (ρ) and conductivity (σ) of the different sintered samples are shown in Table 5. 7 and Figure 5. 8. The resistivity (ρ) and conductivity (σ) of the samples was determined by:

$$\rho = \frac{1}{\omega\epsilon\epsilon''} = \frac{1}{\omega\epsilon\epsilon'\tan\delta}$$

$$\sigma = \frac{1}{\rho}$$

Where ϵ_0 is the free space permittivity, ϵ' is the dielectric constant, ϵ'' is the dielectric loss factor and $\tan\delta$ is the tangent loss. The decrease in resistivity with frequency can be explained by Koop's theorem, which supposed that the dense ceramic material or body acts as a multilayer capacitor. The effect of the multilayer capacitor increases with frequency; as a result, the resistivity decreases [Mazen 2000]. The resistivity increased with zirconia addition due to the reduction in porosity. The presence of pores in the porcelain composition of insulators directly impact or affect the densification of the samples resulting in the decline of efficient loading area and dielectric property. The denser the material, the higher is the mechanical strength. In this point, the density of material plays an important role in the mechanical resistance [Jordan et al. 2008].

Table 5. 7: The dependence of resistivity and conductivity on the frequency (Hz) and addition of zirconia wt. % for the samples sintered at 1350°C.

Freq. (Hz)	Samples sintered at 1350°C									
	D1		D2		D3		D4		D5	
	ρ (10^9 Ω cm)	σ (10^{-10} S cm^{-1})	ρ (10^9 Ω cm)	σ (10^{-10} S cm^{-1})	ρ (10^9 Ω cm)	σ (10^{-10} S cm^{-1})	ρ (10^9 Ω cm)	σ (10^{-10} S cm^{-1})	ρ (10^9 Ω cm)	σ (10^{-10} S cm^{-1})
Where $k=10^3$ and $M=10^6$										
100	8.71	1.15	10.8	0.926	26.1	0.038	6.48	1.54	7.48	0.134
10K	2.74	3.65	3.55	2.82	10.1	0.992	2.66	3.77	5.58	1.79
100K	1.00	9.98	1.39	7.20	2.56	3.91	0.895	11.2	1.57	6.37
1M	0.272	36.8	0.316	31.7	0.417	24.0	0.210	47.6	0.338	29.6

5.3.5.1 AC Dielectric Permittivity and Dielectric Loss at Microwave Frequency (1 to 20 GHz)

As shown in Figure 5. 9, it can be seen that as we increase the content of ZrO_2 (from 0 to 7.5 wt. %), different samples sintered at 1350°C there is an increment in dielectric constant (ϵ'). The dependence of dielectric constant and dielectric loss ($\tan\delta$) on a different frequency at room temperature (Figure 5. 9). It also noted from Figure 5. 9 that, samples sintered at 1350°C having maximum values of dielectric constant is 5.186 at 2.5 GHz and 4.667 for 20 GHz for sample D4 at room temperature. Zirconia has ϵ' of about 27, which is higher than

that of alumina (≈ 10). So as for increasing the zirconia content in the base composition ϵ' goes to increases.

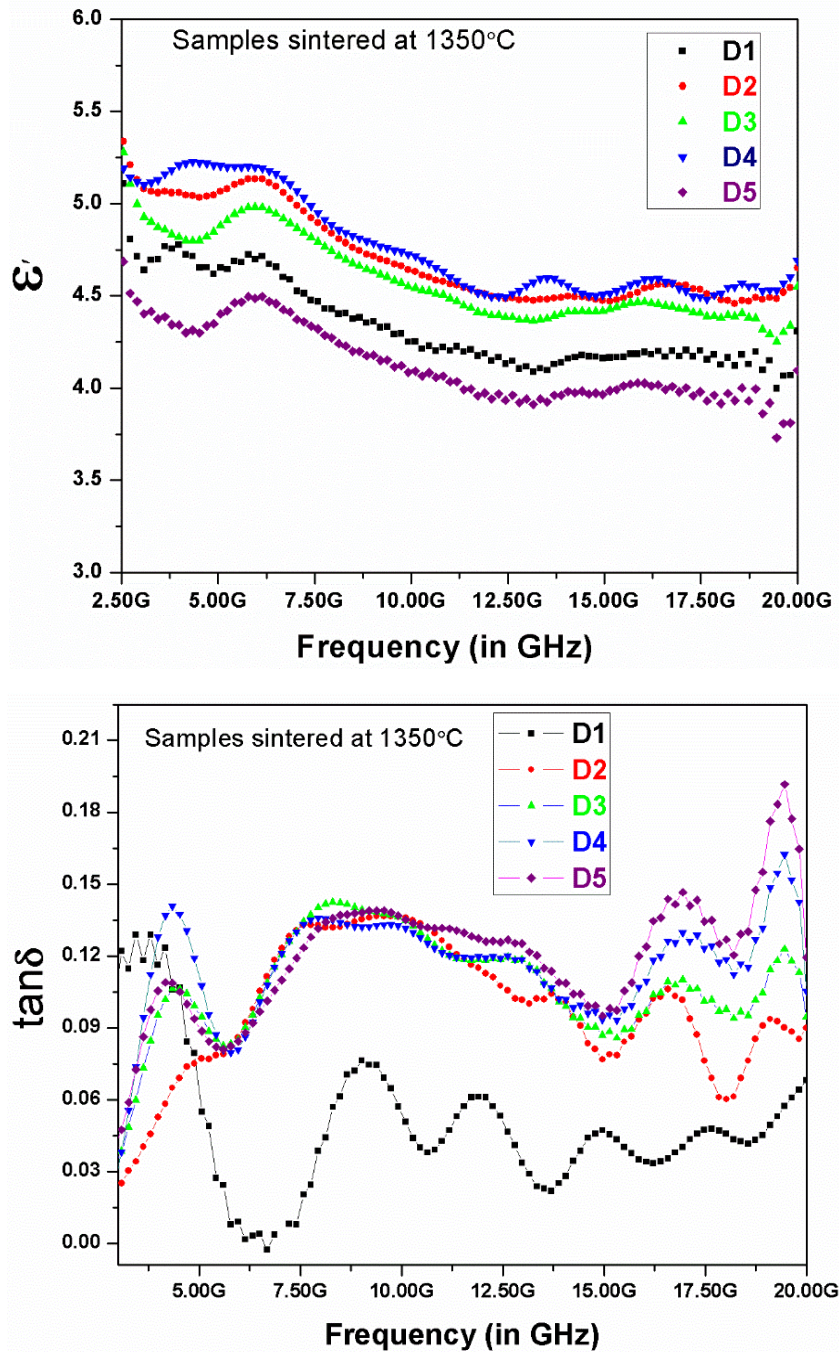
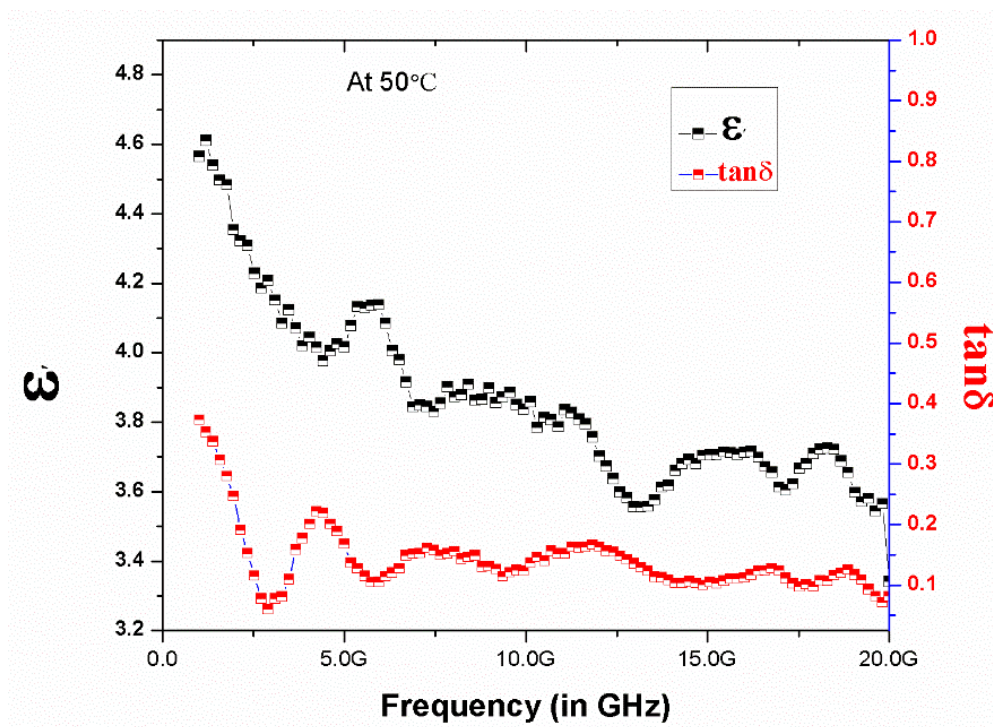


Figure 5. 9: Ac dielectric and loss analysis at microwave frequency with frequency variation up to 20 GHz.

5.3.5.2 AC Dielectric and Loss Analysis at Microwave Frequency with Temperature Variation

From Figure 5. 9 it is noted that, sample D4 having zirconia concentration (7.5 wt. %) in base ceramic porcelain composition shows the maximum value of ϵ' in range of microwave frequency from that of all other samples. So measuring value of ϵ' and dielectric loss for this sample with temperature variation (at 50°C, 150°C and 200°C) as well with frequency variation. From Figure 5. 10, it reveal that value of AC dielectric constant decreasing slowly and the variation in dielectric loss is almost constant. The increase of ϵ' along with temperature because at higher temperature the bonding force between the atoms is decreases.



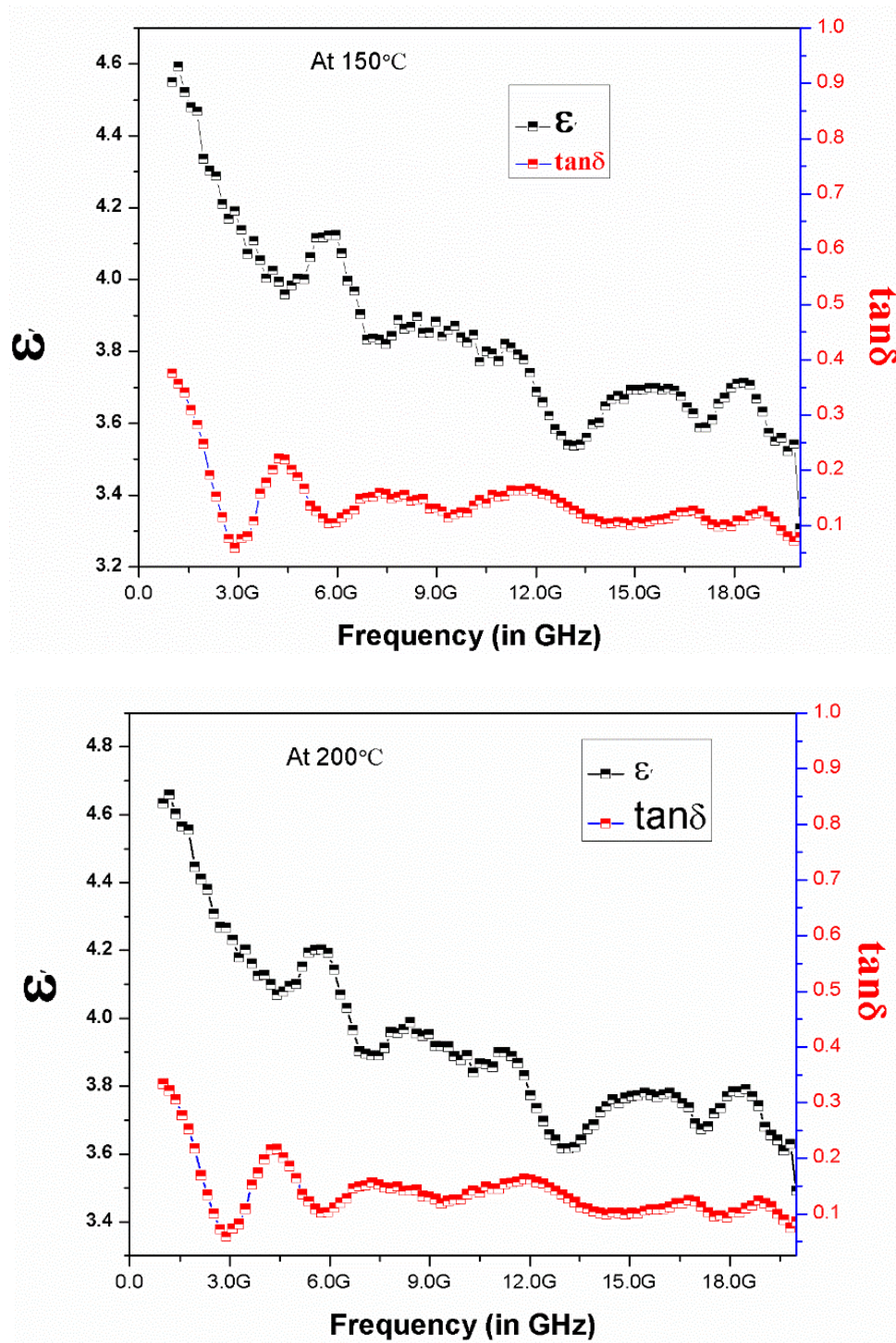


Figure 5. 10: Ac dielectric and loss tangent analysis at microwave frequency with temperature variation (50°C, 150°C and 200°C).

5.3.5.3 AC Dielectric Strength

The average value of five samples of each composition for AC dielectric strength data is shown in Table 5. 8. Figure 5. 11, reveals that the AC dielectric strength of prepared porcelain insulator slightly increases with increase in zirconia content. The relative permittivity of zirconia is near about 27, which is much higher than that of alumina (≈ 10), means having high insulation property. The highest observed AC dielectric strength for samples D4 is 23.96 ± 1 KV/mm, which is sintered at 1350°C . It may be concluded that zirconia as a filler is effective in improving electrical properties.

Table 5. 8: Measurement of dielectric strength of the different samples composition

Sample	Average Breakdown Voltage of five samples (KV)	Average thickness of five samples (mm)	Dielectric Strength (KV/mm)
D1	28	1.39	20.14
D2	29	1.42	20.42
D3	31	1.38	22.46
D4	29	1.21	23.96
D5	26	1.14	22.80

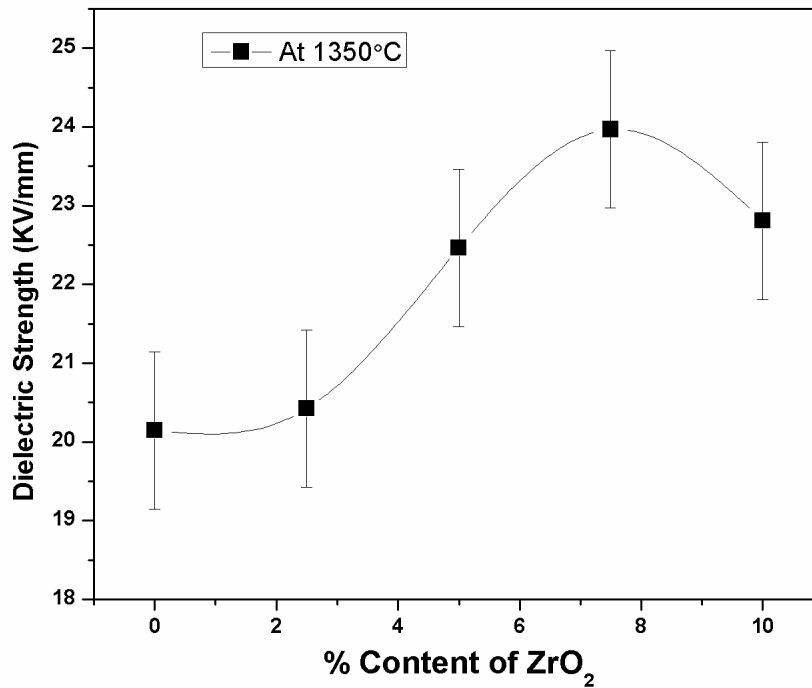


Figure 5. 11: Show the graph for dielectric strength with zirconia content

5.4 Conclusion

A newly developed electrical ceramic porcelain insulator doped with zirconia using economic raw materials was proposed. The selected composition was 25 wt.% kaolin's, 20 wt.% Ball clay, 10 wt.% feldspar, 10 wt.% quartz and 35 wt.% alumina. Additionally, the effect of zirconia (ZrO₂) addition on physical, mechanical and electrical properties of ceramic porcelains insulator was studied. The zirconia addition was responsible for the mechanical and electrical properties improvement in the prepared porcelain insulator. The increases in mechanical properties were mainly related to the residual porosity. The following things were observed when alumina was replaced with zirconia in the base porcelain composition by 7.5 wt. %.

- The bulk density increased and porosity decreased when zirconia content was increased to 7.5% due to the intense bond formation of zirconia, silica, and alumina composite.
- The percentage of water absorbed by the sintered samples decreased because of the decrease in porosity. As the porosity declined, there was less space inside the sample, and it becomes difficult for the water to penetrate inside the body.
- The linear shrinkage showed a steady rise in between from ~8% to 9% due to the densification of the particles as they were sintered at high temperature.
- XRD analysis of the powdered samples confirms the various phases were detected.
- It has been found that the maximum bulk density, the bending, tensile and compressive strength values of porcelains sintered at 1350°C for 2 hours were 2.63 g/cm³, 141±5 MPa, 40±3 MPa and 216±10 MPa, respectively. The difference between compression strength and bending strength was attributed to the difference in stresses distribution in the samples.
- The highest observed AC dielectric strength for samples D4 is 23.96 ± 1 KV/mm, which is sintered at 1350°C.
- The prepared porcelain insulators showed low dielectric losses due to the reduction in eddy current losses. High dielectric constant provides the advantage in power transmission and low dielectric constant used in high-speed electronic circuits (capacitor dielectrics).

If the amount of zirconia is further increased (up to 10%), it was observed that the bulk density and linear shrinkage had a steep fall. At the same time, the porosity and the water absorption in the samples increased. These changes decrease the strength and longevity of

the ceramic porcelain material. Also, zirconia is expensive and using a higher amount of zirconia will not result in the economical availability of the finished product. Studying the results of the various tests, it was concluded that replacing alumina (35 to 27.5 wt. %) with 7.5 wt. % zirconia in the base porcelain composition provided the best results in both physical, mechanical as well as electrical properties of the sintered samples. Nevertheless, the obtained material is suitable for industrial exploitation because of its all these excellent properties.

